Photoswitchable Arene Ruthenium Complexes Containing o-Sulfonamide Azobenzene Ligands

Claire Deo, Nicolas Bogliotti, Rémi Métivier, Pascal Retailleau, Juan Xie

Photoswitchable Arene Ruthenium Complexes Containing *o*-Sulfonamide Azobenzene Ligands

Claire Deo,[†] Nicolas Bogliotti,*[,†] Rémi Métivier,[†] Pascal Retailleau,[‡] and Juan Xie*[,†]

[†] PPSM, ENS Cachan, CNRS, Université Paris-Saclay, 94235 Cachan, France

[‡] Institut de Chimie des Substances Naturelles, CNRS UPR 2301, Univ. Paris-Sud, Université Paris-Saclay, 1, av. de la Terrasse, 91198 Gif-sur-Yvette, France

Supporting Information Placeholder

ABSTRACT: A series of arene ruthenium complexes containing *ortho*-sulfonamide azobenzene ligands were synthesized and found to exhibit uncommon coordination pattern with exocyclic N=N bond. Upon irradiation, these complexes cleanly undergo (*E*)→(*Z*) photoisomerization followed by thermal (*Z*)→(*E*) isomerization (upon resting in the dark) whose rate is dependent on the solvent, the nature of the arene group, sulfonamide moiety and azobenzene substitution, as revealed by structure-property studies.

INTRODUCTION

The photoisomerization properties of azobenzene have been extensively exploited for the control of events at various scales and interfacing many fields such as molecular biology, pharmacology, chemistry, material sciences, physics, information and data storage technology.[1–10] Azobenzene and its derivatives such as 2-(arylazo)pyridines, 2-(arylazo)pyrimidines or 2-(arylazo)imidazoles are also appealing compounds in coordination chemistry due to their interesting redox behavior and the strong M–L bonding resulting from their potent π-acceptor character.[11] Remarkably, these ligands have been frequently combined with ruthenium, and the resulting complexes have found promising applications in catalysis[12–16] or as cytotoxic agents towards various cancer cell lines.[17–20] These compounds most commonly exhibit bidentate or tridentate coordination patterns such as **I**[17–30], **II**[13,16,31,32], **III**[14,15,24,25,32,33] and **IV**[12] (Figure 1). In each case, the N=N bond is located inside a chelate ring formed with the metal, thus preventing azobenzene photoisomerization. Only few exceptions involving multi-metallic species have been shown to maintain photoisomerization ability of azobenzene upon direct coordination of both nitrogen atoms of N=N bond to Ru atom.[34–36] More recent examples concern the photoisomerization of azobenzene-coupled metal complexes without coordination of azobenzene moiety.[37,38]

We reasoned that structural modification of the ligand could affect the coordination pattern in such a way that the photoswitching ability of azobenzene would be maintained upon coordination to the metal center. The resulting organometallic complexes could be interesting candidates for the photocontrol of catalytic activity[39–44] and biological applications.[1,3,5,9,45–47] Here, we wish to report a new type of photoswitchable arene-ruthenium complexes containing *o*-sulfonamide azobenzenes as ligands (**V**, Figure 1) and describe their photoisomerization properties.

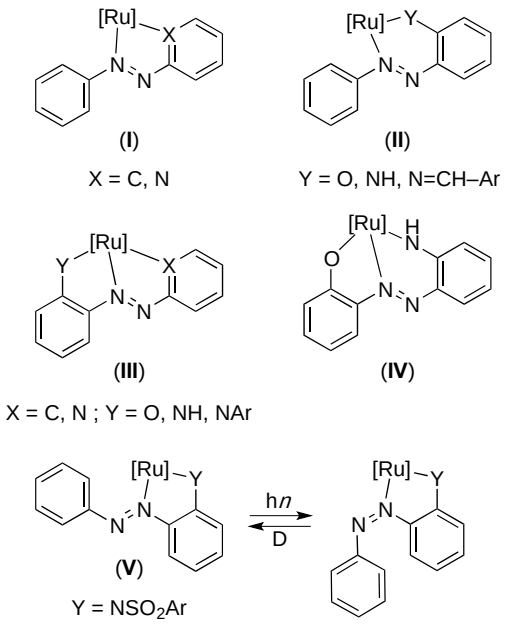

Figure 1. Common coordination pattern for ruthenium-azobenzene complexes (**I**-**IV**) and novel type of photoswitchable organometallic complexes (**V**).

RESULTS AND DISCUSSION

Synthesis and photophysics of ligand 3 and complex 4. Prototype *ortho*-tosylamide azobenzene **3**[48] was synthesized as described in Scheme 1 in order to investigate

its behavior as a ligand for ruthenium. Commercially available *o*-phenylenediamine was tosylated under standard conditions (TsCl, pyridine) to yield 91% of **1**[49], which underwent reaction with Oxone® to afford *o*-tosylaminonitrosobenzene **2** in 94% yield. This compound was treated under Mills conditions,[8] in the presence of aniline and acetic acid in refluxing toluene, to give the desired *o*-tosylaminoazobenzene ligand **3**. Finally, reaction with ruthenium dimer $[Ru(p\text{-cym})Cl_2]_2$ and triethylamine in methanol led to ruthenium complex **4** as a dark brown solid (78% yield). The structure of this complex was confirmed by ^{1}H- and ^{13}C-NMR spectroscopy, HRMS and elemental analysis. Crystals suitable for X-ray crystallographic analysis were obtained by slow evaporation of a solution of the complex in CH_2Cl_2. The structure of complex **4** reveals a classical "three-legged piano-stool" configuration at ruthenium atom, and most importantly, **3** acts as a bidentate *N,N*-ligand forming a five-membered ring with exocyclic N=N bond (Figure 2 and discussion below).

Scheme 1. Synthesis of ligand **3** and complex **4**

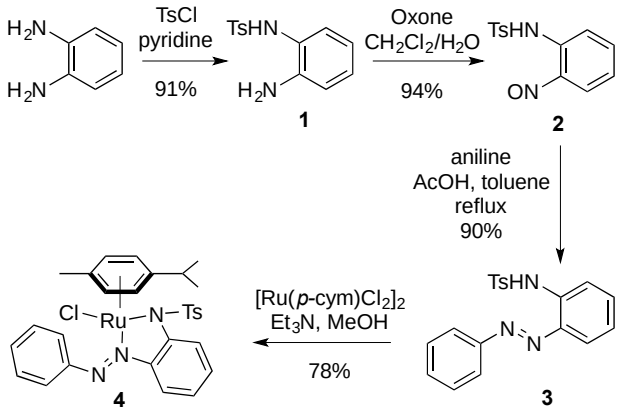

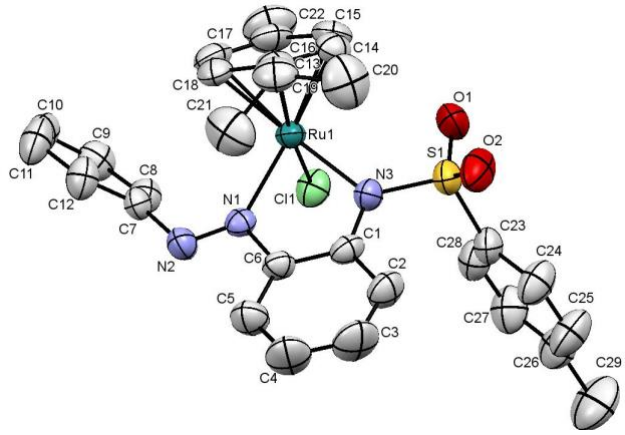

Figure 2. ORTEP representation (thermal ellipsoids drawn at 50% probability level) of complex **4** with atom numbering scheme. The hydrogen atoms have been omitted for clarity. Selected bond lengths (Å) and angles (deg): Ru–N1 = 2.081(2), Ru–N3 = 2.101(2), Ru–Cl1 = 2.3993(8), Ru–cent = 1.703(3), N1–N2 = 1.258(3), N3–S1 = 1.618(2); N3–Ru–Cl1 = 85.65(7), N3–Ru–N1 = 77.57(9), N1–Ru–Cl1 = 86.46(6).

Preliminary spectroscopic and photophysical studies of ligand **3** and complex **4** were performed in MeCN. Free ligand **3** exhibits a strong absorption band at 324 nm (ε = 16650 ± 350 L.mol^{-1}.cm^{-1}) assigned to π→π* transition and a weak band at 454 nm (ε = 800 ± 10 L.mol^{-1}.cm^{-1}) corresponding to a forbidden n→π* transition (black line, Figure 3). Complex **4** shows two bands of similar intensity at 319 nm (ε = 9550 ± 20 L.mol^{-1}.cm^{-1}) and 421 nm (ε = 6850 ± 30 L.mol^{-1}.cm^{-1}), both assigned mainly to intraligand π→π* transitions, and a weaker band in the visible region at 566 nm (ε = 2750 ± 20 L.mol^{-1}.cm^{-1}) assigned mainly to Ru ($4d^6$)→π* transition (black line, Figure 4).[20]

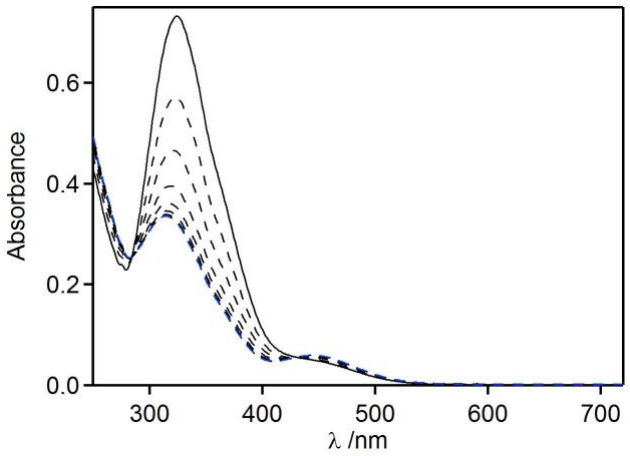

Figure 3. Absorption spectrum of ligand (*E*)-**3** in MeCN (C = 45 µM) at 25°C (bold line) and its stepwise evolution upon 5 sec irradiation pulses at 315 nm with P = 40 mW.cm^{-2} (dashed lines). Blue dashed line corresponds to PSS.

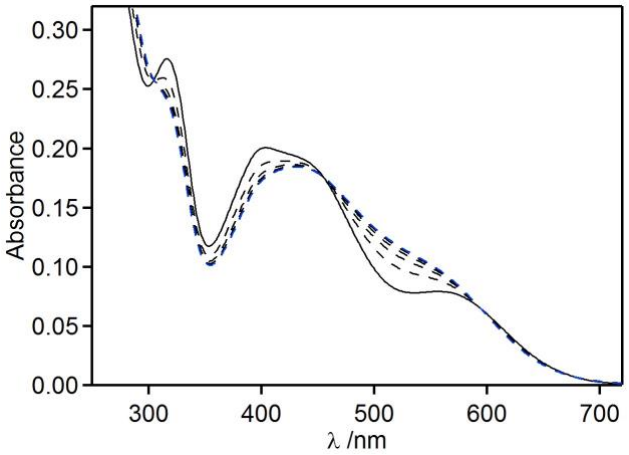

Figure 4. Absorption spectrum of ruthenium complex (*E*)-**4** in MeCN (C = 30 µM) at 25°C (black line) and its stepwise evolution upon 5 sec irradiation pulses at 406 nm with P = 9 mW.cm^{-2} (dashed lines). Blue dashed line corresponds to PSS.

Scheme 2. Photoswitching of ligand **3** and complex **4**.

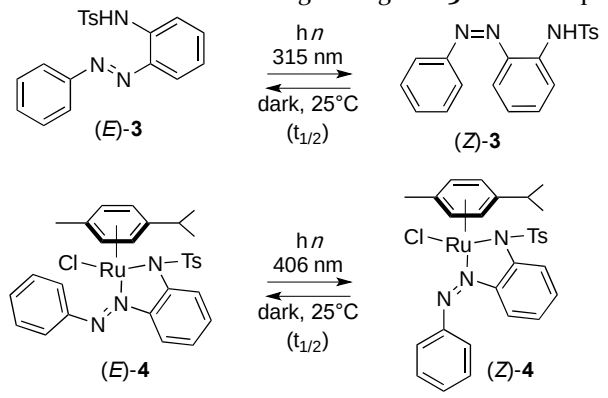

As expected, irradiation at 315 nm of a solution of **3** in MeCN resulted in a steady decrease of the band at 324 nm, with two isosbestic points at 285 and 422 nm, revealing (*E*)→(*Z*) photoisomerization of azobenzene moiety (Figure 3 and Scheme 2). Under these conditions, photostationary state (PSS) was reached after *ca*. 35 s. Its composition was determined to be (*E*) : (*Z*) = 29 : 71 by a combination of ^{1}H-NMR and UV-Vis spectroscopy (see Supporting Information for details). The half-life of (*Z*)-**3** (determined upon resting the sample in the dark at 25°C) could not be precisely measured due to reproducibility issues, but several independent experiments indicated $t_{1/2}$(*Z*) values ranging from 1 h to 4 h in MeCN. Similar behavior has already been reported for other azobenzene derivatives such as azopyridines, and was attributed to their high sensitivity to traces of water or acid.[50] Attempts to buffer solution of **3** in MeCN either by addition of 1% (v/v) H_2O at pH 7, or 1‰ (v/v) TFA greatly shortened the half-lives of the (*Z*)-isomer without improving reproducibility ($t_{1/2}$ around 240 s and 30 s, respectively).

Gratifyingly, complex **4** also undergoes photoisomerization upon irradiation at 406 nm in MeCN as revealed by concomitant steady decrease of absorption band around 400 nm and increase around 515 nm, and the presence of an isosbestic point at 456 nm (Figure 4 and Scheme 2). PSS was rapidly reached (in *ca*. 35 s), and a ratio (*E*) : (*Z*) = 56 : 44 was determined by the same method as for ligand **3** (see Supporting Information). The rate of thermal back (*Z*)→(*E*) isomerization was determined to be much faster than in the case of **3**, with reproducible $t_{1/2}$ value of 6.5 ± 0.3 min at 25°C in MeCN. Noteworthy is the fact that such a switching process could be repeated over ten times without any noticeable degradation of the complex (Figure 5).

Photoisomerization study of 4 by ^{1}H-NMR spectroscopy. A portion of the ^{1}H-NMR spectra of **4** in CD_3CN before and after irradiation is reported in Figure 6. The aromatic protons of the *p*-cymene moiety appear as four distinct signals: two doublets at 5.43 and 5.05 ppm corresponding to H14 and H15, and two broad signals at 6.21 and 3.51 ppm, corresponding to H18 and H17, respectively (Figure 6). This significant perturbation of chemical shifts can be explained by the influence of the aryl group of azobenzene directly facing the *p*-cymene moiety (Figure 2), and resulting in a strong shielding of H17 (*ca*. 1.5 ppm) located above the aromatic ring, and deshielding of H18 (*ca*. 1 ppm) located on the side of the ring (Figure 6). Irradiation of (*E*)-**4** at 406 nm resulted in the apparition of a new set of signals corresponding to (*Z*)-**4**. As a consequence of isomerization of the N=N bond, the aryl group of azobenzene does not exert any ring current effect, the *p*-cymene group in (*Z*)-**4** thus appears as four well-defined doublets between 5.42 and 5.99 ppm (green arrows).

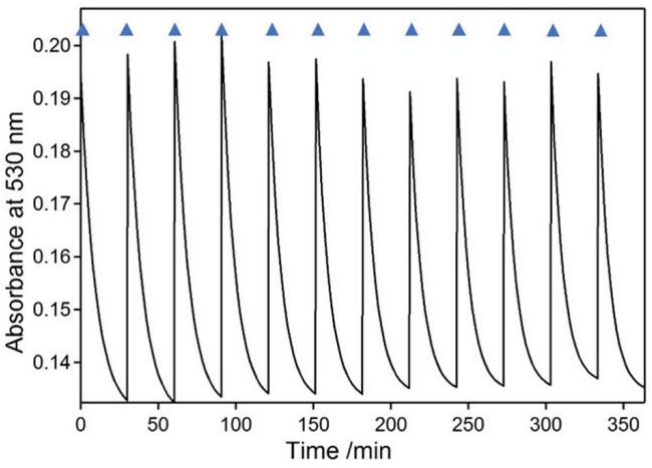

Figure 5. Fatigue resistance of complex **4** in MeCN (C = 60 µM) upon alternating irradiation and resting (dark, 25°C). Blue triangles refer to irradiation pulses at 406 nm.

Structure-property relationship in arene ruthenium *o*-sulfonamide azobenzenes. Encouraged by these results, we decided to prepare other complexes, in order to investigate the influence of structure on photophysical properties. We focused on i) changing the nature of sulfonamide group, ii) introducing fluorine atoms on the benzene group, as such a modification is known to result in very long-lived (*Z*) isomers[51,52] and iii) modifying arene ligand on ruthenium (Figure 7).

The synthesis of complexes **7** and **9** is described in Scheme 3. Nitrosobenzene was treated with *o*-phenylenediamine under classical Mills conditions in the presence of acetic acid in refluxing toluene, to afford amino azobenzene **5** in 46% yield.[53] Treatment with MsCl and pyridine in dichloromethane gave ligand **6**, which was easily converted to complex **7** in 63% yield upon reaction with $[Ru(p\text{-cym})Cl_2]_2$ and triethylamine in methanol. Reaction of **5** with triflic anhydride in CH_2Cl_2 yielded 94% of ligand **8** which was converted to complex **9**, in the presence of $[Ru(p\text{-cym})Cl_2]_2$ in MeOH.

Initial attempts to react commercially available 2,6-difluoroaniline with nitroso derivative **2** did not lead to the expected fluorinated ligand **11** (Scheme 4). However, when 2,6-difluoroaniline was transformed into the corresponding nitroso compound **10**, followed by reaction with amine **1**, ligand **11** was obtained in 24% yield. Then, formation of difluorinated complex **12** proceeded smoothly as described for **4** and **7**.

Modification of the aryl group has been shown previously to significantly affect the properties and reactivity of ruthenium arene complexes.[54,55,20,56–59] However, to the best of our knowledge, its influence on the isomerization properties of azobenzene ligands has never been investigated. Thus, we synthesized complexes **13** and **14**, analogous to **4**, in which the *p*-cymene ligand is replaced by benzene and hexamethylbenzene, respectively (Scheme 5). Standard reaction conditions, using $[Ru(C_6H_6)Cl_2]_2$ or $[Ru(C_6Me_6)Cl_2]_2$ and ligand **3** in the presence of Et_3N in

MeOH cleanly afforded the desired complexes in 83% and 75% yield as dark brown solids.

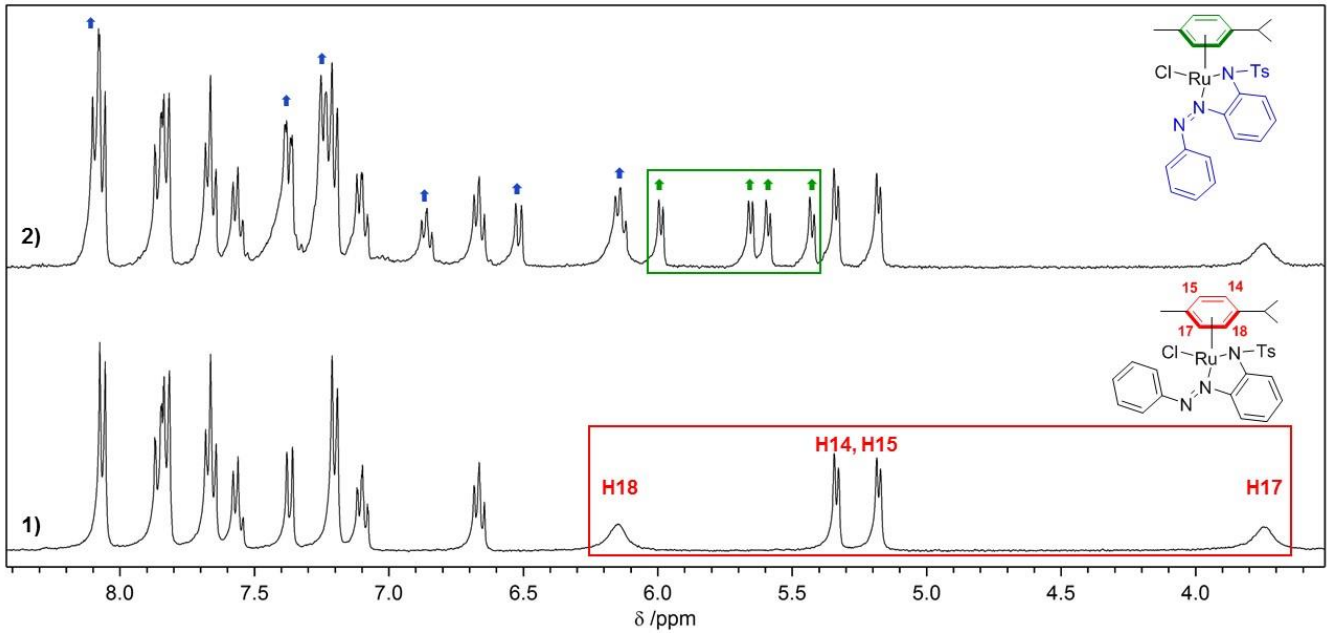

Figure 6. Portions of ^{1}H-NMR spectra of complex **4** in CD_3CN (C = 13 mM): 1) before irradiation and 2) after irradiation at 406 nm (P = 40 mW.cm^{-2}, t = 15 min). The red and green frames indicate the signals corresponding to the aromatic protons of the *p*-cymene moiety of (*E*) and (*Z*) isomers, respectively; arrows indicate the signals corresponding to the (*Z*) isomer appearing upon irradiation.

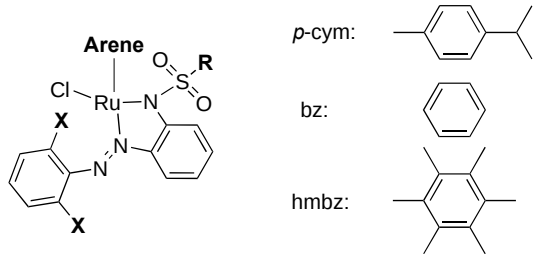

Compound	Arene	R	X
4:	*p*-cym	—Me	H
7:	*p*-cym	—Me	H
9:	*p*-cym	—CF_3	H
12:	*p*-cym	—Me	F
13:	bz	—Me	H
14:	hmbz	—Me	H

Figure 7. Ruthenium-arene complexes investigated for structure-property relationship.

Scheme 3. Synthesis of ligands **6** and **8**, and their corresponding complexes **7** and **9**.

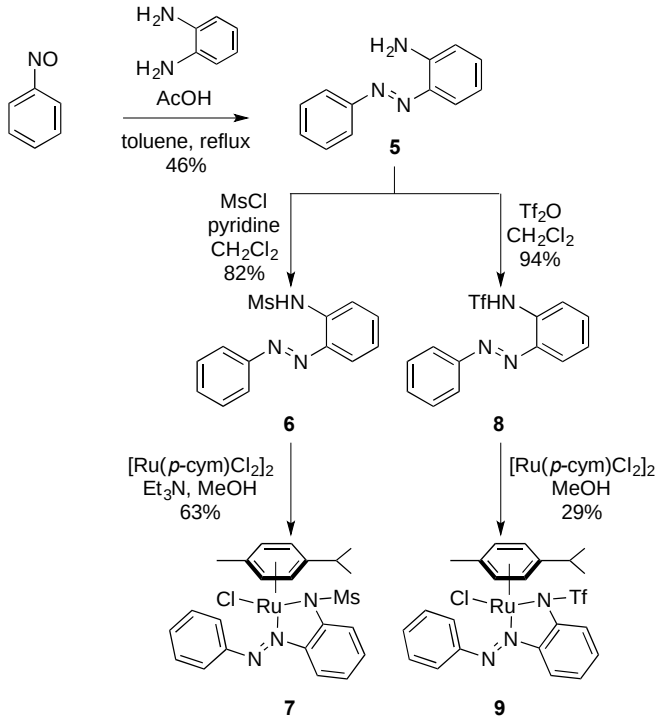

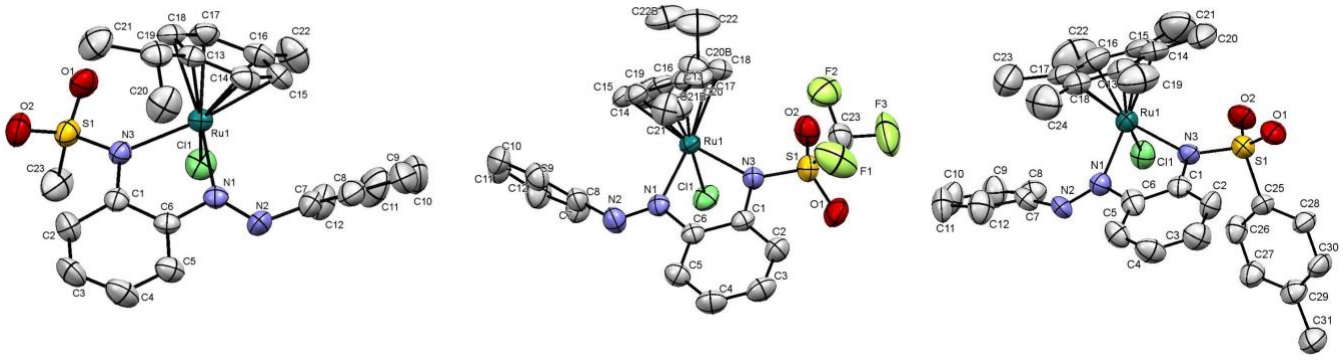

Figure 8. ORTEP representation (thermal ellipsoids drawn at 50% probability level) of complexes **7** (left), **9** (middle) and **14** (right) with atom numbering scheme. The hydrogen atoms and solvent molecule (for **14**·CH_2Cl_2) have been removed for clarity.

Scheme 4. Synthesis of fluorinated ligand **11** and complex **12**.

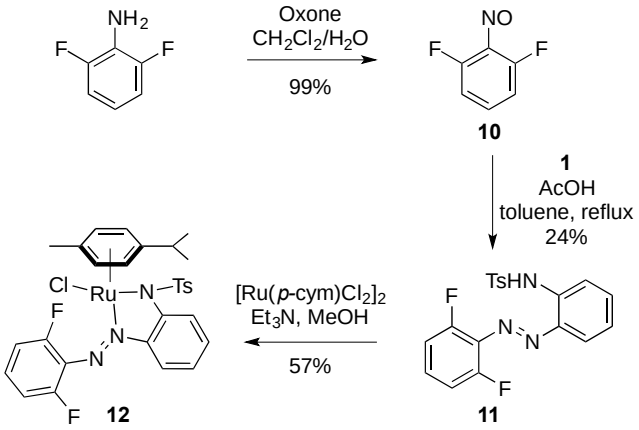

Scheme 5. Synthesis of benzene and hexamethylbenzene complexes **13** and **14**.

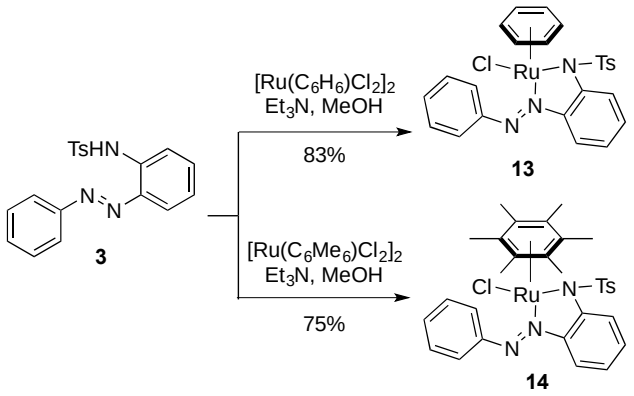

The molecular structures of the ruthenium complexes **4**, **7**, **9** and **14** were determined by single crystal X-ray diffraction. Their representations along with atom numbering scheme are shown in Figure 2 and Figure 8, and selected bond lengths and angles are listed in Table 1. Complexes **4**, **7**, **9** and **14** share similar structures, with ruthenium center in a pseudo-octahedral geometry in which the η^6-arene ligand occupies a face. The ruthenium-arene centroid distances (in the range between 1.702 and 1.714 Å) and Ru-N(1) distances (from 2.081(2) to 2.10(2) Å) are comparable to those reported for other arene-ruthenium complexes containing azobenzene ligands.[16,20,27] It should be noticed that the (*E*)-azo-ligands do not adopt a planar geometry after coordination. The angle between the planes of the two aromatic groups of azobenzene are nearly identical in compounds **4** and **7** (θ = 57.38° and 54.96°, respectively), while this value is higher in **9** (68.27°) and significantly reduced in **14** (30.83°). Interestingly, the X-Ray structure of **9** shows a component of disorder around the isopropyl group of the *p*-cymene moiety.

Table 1. Selected bond lengths (Å) and angles (deg) for complexes **4**, **7**, **9** and **14**.

	4	**7**	**9**	**14**
Ru-N(1)	**2.081(2)**	**2.090(5)**	**2.093(2)**	**2.10(2)**
Ru-N(3)	**2.101(2)**	**2.104(5)**	**2.132(3)**	**2.12(1)**
Ru-Cl(1)	**2.3993(8)**	**2.405(2)**	**2.398(1)**	**2.404(5)**
Ru-cent[a]	**1.703**	**1.714**	**1.702**	**1.710**
N(1)-N(2)	**1.258(3)**	**1.255(6)**	**1.263(3)**	**1.28(3)**
N(3)-S(1)	**1.618(2)**	**1.631(6)**	**1.590(3)**	**1.63(2)**
N(3)-Ru-Cl(1)	**85.65(7)**	**85.6(1)**	**85.06(8)**	**88.7(4)**
N(3)-Ru-N(1)	**77.57(9)**	**78.0(2)**	**78.0(1)**	**77.4(6)**
N(1)-Ru-Cl(1)	**86.46(6)**	**88.7(1)**	**87.32(8)**	**94.5(5)**
θ[b]	**57.38**	**54.96**	**68.27**	**30.83**

[a] cent = centroid of arene moiety. [b] θ = angle between the planes of the two aromatic rings of azobenzene ligand.

The ^{1}H-NMR spectra of **4**, **7**, **9**, **12**, **13** and **14** in $CDCl_3$ revealed well-defined signals corresponding to the

azobenzene ligand, while signals related to the *p*-cymene moiety showed great differences in complexes **4**, **7**, **9** and **12**. In **4** and **7**, *p*-cymene exhibits characteristic signals for aromatic protons: two doublets in the range 5.43-5.33 and 5.05-5.02 ppm, and two broad signals at 6.32-6.20 and 3.74-3.51 ppm, as a consequence of the strong ring current effect exerted by azobenzene ligand (see Figure 6, Supporting Information and discussion above), while the *i*-Pr group appears as a septuplet at 2.67-2.56 ppm and two doublets at 1.08-1.07 and 0.89-0.87 ppm, and the Me group appears as a singlet at 2.15-2.11 ppm. The ^{1}H-NMR spectrum of **12** shows broad signals corresponding to aromatic protons above 6.5 ppm (1H), around 5.5 ppm (2H) and around 3.7 ppm (several signals corresponding to 1H). The *i*-Pr group appears as broad signals at 2.83, 1.19 and 0.87 ppm, and the Me group as a broad signal at 1.99 ppm. The pattern exhibited by *p*-cymene in **9** is slightly different, with seven broad signals appearing between 6.03 and 3.98 ppm (aromatic protons), around 2.50 and 1.00 ppm (*i*-Pr group) and in the range 2.39-2.08 ppm (Me group). The observation of such broad signals for **12** and **9** presumably indicate their existence as slowly-interconverting conformers in solution, consistent with the disorder observed around the *i*-Pr group of **9** in the solid state. The signals of the arene group of **13** and **14** appear as singlets at 5.48 and 1.83 ppm, respectively.

The spectroscopic properties of the synthesized complexes in MeCN were compared, and are summarized in Table 2. Compounds **4**, **7**, **9**, **12** and **13** displayed similar absorption spectra (Figure 4 and Supporting Information), with two bands around 314-319 nm and 390-454 nm that can be assigned to the π→π* intra-ligand transition, and one band around 514-586 nm with a lower extinction coefficient that can be assigned to the MLCT (metal-ligand charge transfer) transition from the 4d orbitals of Ru(II) to the empty π* ligand orbitals (Table 2). As a plausible consequence of the singular geometry of **14** as compared to other complexes, this compound exhibited a notably different pattern with three intense bands at 319 nm, 394 nm and 485 nm assigned to π→π* intra-ligand transition, and a broad band around 617 nm corresponding to MLCT transition (Figure 9). As previously described for **4**, irradiation at 406 nm of complexes **7**, **9**, **12**, **13** and **14** in MeCN induced photoizomerisation of the ligand, as revealed by the decrease of absorption band at 390-454 nm and increase around 500-550 nm (Figure 9 and Supporting Information).

Table 2. Electronic spectral data and transition assignment for complexes **4**-**14** in CH_3CN.

Compound	λ	ε /L.mol^{-1}.cm^{-1}	Transition
4	**319 nm**	**9574 ± 21**	**π→π***
	421 nm	**6850 ± 24**	**π→π***
	566 nm	**2740 ± 14**	**MLCT**
7	**315 nm**	**7729 ± 28**	**π→π***
	400 nm	**5516 ± 15**	**π→π***
	560 nm	**2231 ± 27**	**MLCT**
9	**314 nm**	**7395 ± 88**	**π→π***
	390 nm	**5437 ± 60**	**π→π***
	514 nm	**1621 ± 50**	**MLCT**
12	**317 nm**	**7400 ± 28**	**π→π***
	454 nm	**5448 ± 53**	**π→π***
	586 nm	**1847 ± 34**	**MLCT**
13	**316 nm**	**8133 ± 11**	**π→π***
	444 nm	**5022 ± 26**	**π→π***
	556 nm	**2604 ± 45**	**MLCT**
14	**319 nm**	**6842 ± 21**	**π→π***
	394 nm	**8557 ± 38**	**π→π***
	485 nm	**5872 ± 15**	**π→π***
	617 nm	**1719 ± 40**	**MLCT**

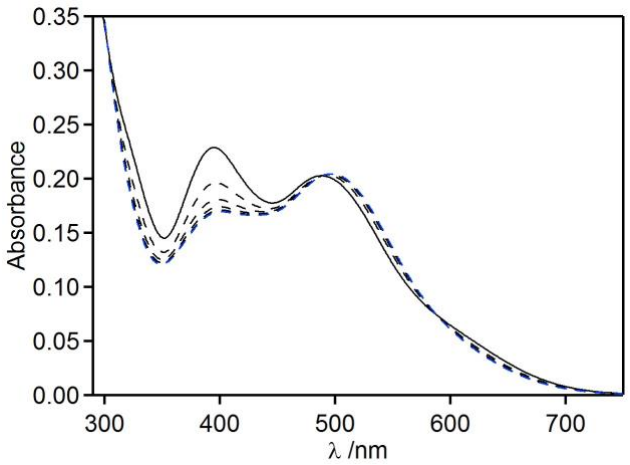

Figure 9. Absorption spectrum of ruthenium complex (*E*)-**14** in MeCN (C = 30 μM) at 25°C (black line) and its stepwise evolution upon 5 sec irradiation pulses at 406 nm with P = 9 mW.cm^{-2} (dashed lines). Blue dashed line corresponds to PSS.

Solvent effects on thermal (*Z*)→(*E*) isomerization rates of complexes. In order to assess the influence of solvent on isomerization properties of the synthesized complexes, solutions of **4**, **7**, **9**, **12**, **13** and **14** in solvent with varying polarity (toluene, THF, CH_2Cl_2, acetone, MeCN and EtOH), were prepared. Irradiation at 406 nm cleanly triggered (*E*)→(*Z*) photo-isomerization, then half-life of (*Z*)-isomer (rate of thermal back-reaction) was determined by monitoring evolution of absorbance at appropriate wavelength (see Supporting Information for details). The results are reported in Table 3. For most complexes studied, $t_{1/2}(Z)$ increases with increasing solvent polarity (as evaluated by the empirical polarity scale E_T^N)[60], ranging from 0.66 min to 3.68 min in toluene (E_T^N=0.099) to 3.48 to 33.6 min in EtOH (E_T^N=0.654). Noteworthy is the case of CH_2Cl_2 (E_T^N=0.309), which, although slightly less polar than acetone (E_T^N=0.355) results in longer $t_{1/2}(Z)$ values. The

general trends observed can be understood in term of a better solvation of (*Z*)-complexes (exhibiting a higher permanent dipole than (*E*)-isomers) in polar solvents, thus increasing their thermal stability and consequently the $t_{1/2}(Z)$ values.[51,61,62]

Table 3. Half-Lives ($t_{1/2}$, min) of (*Z*) Isomers of Complexes **4**-**14** in Various Solvents (Ranked by Order of Increasing Polarity Parameter E_T^N)[a]

Entry	Solvent	E_T^N	4	7	9	12	13	14
1	Toluene	0.099	1.50 ± 0.01	0.66 ± 0.01	3.68 ± 0.01	1.21 ± 0.01	2.26 ± 0.03	2.33 ± 0.02
2	THF	0.207	2.65 ± 0.01	1.12 ± 0.01	5.05 ± 0.02	2.38 ± 0.01	2.63 ± 0.09	3.78 ± 0.03
3	CH_2Cl_2	0.309	5.55 ± 0.02	2.85 ± 0.02	6.51 ± 0.01	7.02 ± 0.10	4.82 ± 0.57	18.3 ± 0.1
4	Acetone	0.355	5.44 ± 0.02	2.26 ± 0.01	5.67 ± 0.01	5.23 ± 0.02	4.28 ± 0.88	10.9 ± 0.1
5	MeCN	0.460	6.46 ± 0.31	2.33 ± 0.01	10.1 ± 0.1	8.11 ± 0.03	2.26 ± 0.36	26.5 ± 0.2
6	EtOH	0.654	7.29 ± 0.05	3.48 ± 0.02	n.d.[b]	11.8 ± 0.5	6.45 ± 0.25	33.6 ± 0.3

[a] (*Z*) isomers were formed by irradiation at 406 nm (P = 9 mw.cm^{-2}) for 20 sec, then thermal back isomerization was followed by monitoring UV/Vis absorption in the dark at 25°C. [b] n.d.: not determined (unstable in EtOH).

While *o*-fluoroazobenzenes are well known to exist as very long-lived (*Z*)-isomers (with half-lives reaching more than 2 years),[51,52] $t_{1/2}(Z)$ value for **12** is in the timescale of several minutes as other Ru-complexes. Although the factors responsible for such a behavior could not be precisely identified yet, it is likely that coordination of azobenzene to the metal center affected the π-conjugation structure and the increment in the dipole moment.[37] Besides, conformational change of azobenzene ligand associated with Ru-coordination led to an increase of angle between the planes of the two aromatic rings (Table 1) which might facilitate the (*Z*)→(*E*) thermal isomerization. Interestingly, the nature of sulfonamide group exerts a significant effect on the rate of (*Z*)→(*E*) thermal isomerization, with (*Z*)-**9** (Tf group) showing longer half-life than (*Z*)-**4** (Ts group) and (*Z*)-**7** (Ms group). The Hammet constant *F*, recognized as a good quantification of inductive withdrawing effect of a substituent, parallels this observation: the most electron withdrawing group Tf (F = 0.74[63]) indeed shows longer $t_{1/2}(Z)$ value, than Ts (F = 0.55[64]) and Ms (F = 0.54[35]). Finally, the most striking aspect concerning structure-property relationship in our complexes is the influence of the arene group on the isomerization.

Comparison of **4**, **13** and **14** clearly revealed a strong effect of the presence of hexamethylbenzene ligand on the half-life of (*Z*)-isomer. Indeed, while **4** and **13** exhibited similar $t_{1/2}(Z)$ values ranging from 1.50 to 7.29 min depending on the solvent, $t_{1/2}(Z)$ for **14** varied between 2.33 and 33.6 min. In order to understand the origin of such a difference, the geometry of both (*E*) and (*Z*)-isomers of complexes **4**, **13** and **14** was optimized by DFT calculations using Gaussian 09[65] at the B3LYP/6-31G**(d,p);LanL2DZ[Ru] level and CPCM model for MeCN (Figure 10). All three (*E*)-isomers exhibit similar geometry, with an angle between the planes of the two aromatic rings of azobenzene ligand (θ) of 55.07°, 50.79° and 33.49° for **4**, **13** and **14**, respectively. These results are in good agreement with the θ values determined for **4** (57.38°) and **14** (30.83°) in the solid state by X-Ray analysis (see Table 1). Interestingly, although (*Z*)-**4** and (*Z*)-**13** exhibit similar geometry (θ = 64.26° and 62.17°, respectively) the relative orientation of phenyl rings in azobenzene (*Z*)-**14** is reversed, leading to a θ value of –64.62°. Such observation is presumably the result of two phenomena: i) steric interactions exerted by the methyl groups of hmbz ligand on the phenyl ring of azobenzene; ii) change in the polarity of (*E*) and (*Z*) complexes and their HOMO energy as a consequence of electron enrichment of the metal center by hmbz ligand.

CONCLUSION

A novel series of arene ruthenium complex containing *ortho*-sulfonamide azobenzene ligands were synthesized and characterized. The unusual coordination pattern exhibited by the N=N bond of azobenzene ligand, which was found to be exocyclic, allowed the preservation of its photoisomerization properties thus leading to photoswitchable organometallic complexes. Compared to uncoordinated azobenzene ligands, the corresponding Ru complexes favored the (*Z*)→(*E*) thermal isomerization. The influence of solvent and structural parameters, such as substituents on the phenyl ring of azobenzene, nature of

sulfonamide group and arene ligand, on the rate of thermal (*Z*)→(*E*) back isomerization was investigated, and the presence of hexamethylbenzene group on ruthenium was found to significantly increase half-life of the corresponding (*Z*)-isomer. On the basis of DFT calculations, this effect was rationalized by steric interactions between the arene ligand and the phenyl ring of azobenzene. With these novel photoswitchable organometallic complexes with well-defined properties in hand, our current efforts are focused to the study of their reactivity.

EXPERIMENTAL SECTION

General Procedures. Unless otherwise stated, all reagents were used as received without further purification. Manipulations in anhydrous conditions were carried out under an atmosphere of argon in dried glassware. Solvents were dried with a mBraun MB-SPS-800 purification system. ^{1}H and $^{13}C\{^{1}H\}$ NMR spectra were recorded on a JEOL 400 spectrometer and referenced to the resonances of solvent residual peak. Infrared (IR) spectra were recorded with a Nicolet Nexus FT-IR spectrometer equipped with an ATR-Germanium unit and are reported as wavenumbers (cm^{-1}). Melting points were determined using a Kofler bench. High-resolution mass spectra (HRMS) were performed on a Bruker maXis Q-TOF mass spectrometer by the "Fédération de Recherche" ICOA/CBM (FR2708) platform. Elemental analyses were carried out by the Laboratory for Microanalysis at ICSN (Gif-sur-Yvette). Crystals suitable for X-Ray analysis were obtained either by slow evaporation of a solution of the complexes in CH_2Cl_2 or by slow vapor diffusion of petroleum ether in a solution of the complexes in CH_2Cl_2.

Spectroscopic Measurements. Acetonitrile, acetone, dichloromethane, ethanol, toluene and THF used for absorption measurements were of spectrometric grade. Dichloromethane was passed through a neutral alumina column prior to use to avoid any acidic catalysis. UV/Vis absorption spectra were recorded on a Cary5000 spectrophotometer from Agilent Technologies. Photoisomerization was induced by a continuous irradiation Hg/Xe lamp (Hamamatsu, LC6 Lightningcure, 200 W) equipped with narrow band interference filters of appropriate wavelengths (Semrock FF01-315/15-25 for λ_{irr} = 315 nm; FF01-406/15-25 for λ_{irr} = 406 nm). The irradiation power was measured using a photodiode from Ophir (PD300-UV).

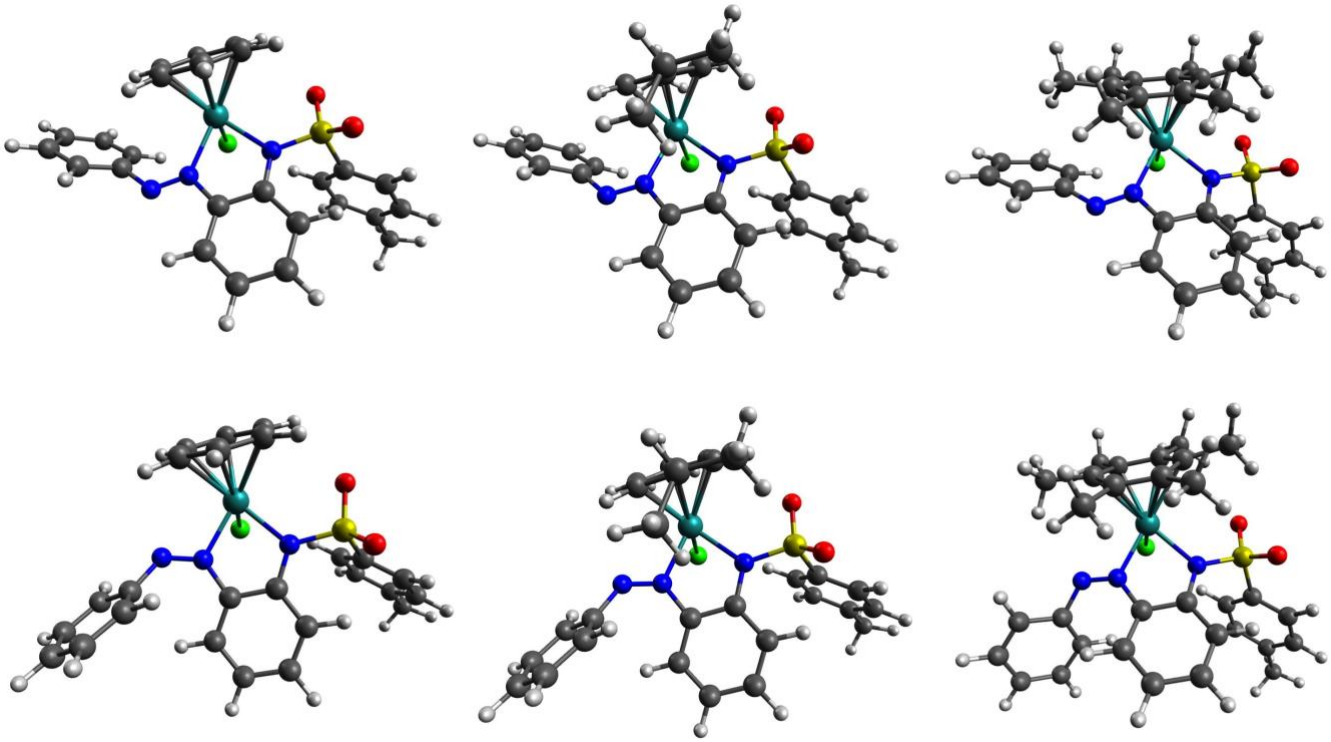

Figure 10. DFT-optimized geometries for (*E*)- (top) and (*Z*)-isomers (bottom) of complexes **13** (left), **4** (middle) and **14** (right).

***N*-(2-Nitrosophenyl)-4-methylbenzenesulfonamide 2.** To a solution of **1**[49] (100 mg, 0.362 mmol) in CH_2Cl_2 (5 mL) was added dropwise a solution of Oxone® (281 mg, 0.457 mmol, 1.2 eq) in 5 mL of H_2O. The resulting mixture was vigorously stirred at room temperature for 24 h. The layers were separated and the aqueous layer was extracted with CH_2Cl_2 (2 × 5 mL). The organic layers were combined, washed with brine, dried over anhydrous sodium sulfate and evaporated under vacuum to afford **2** (99 mg, 0.36 mmol, 94%). Green crystalline solid; R_f: 0.35 (petroleum ether/ethyl acetate: 8/2); Mp: 135°C; IR: 3662, 3227, 2986, 2902, 1624, 1597, 1492, 1320, 1164, 1127, 915, 819, 763, 684 cm^{-1}; ^{1}H NMR (400 MHz, $(CD_3)_2CO$): δ 10.81 (br s, 1 H), 7.93 (d, J = 8.2 Hz, 1H), 7.85 (d, J = 8.2 Hz, 2H), 7.76 (m, 1H), 7.33 (d, J = 8.2 Hz, 2H), 7.15 (t, J = 7.6 Hz, 1H), 6.71 (d, J = 7.3 Hz, 1H), 2.33 (s, 3H); $^{13}C\{^{1}H\}$ NMR (100 MHz, $(CD_3)_2CO$): δ 158.1, 145.5, 139.7, 139.5, 137.7, 130.8, 128.4, 124.3, 122.3, 114.0, 21.5; HRMS (ESI) calcd. for $C_{13}H_{12}N_2O_3SK^+$, $[M + K]^+$ m/z 315.0200, found m/z 315.0198.

(*E*)-2-(4-Methylphenylsulfonamido)azobenzene **3**.[66] To a solution of aniline (100 µL, 1.10 mmol) in toluene (20 mL) were added acetic acid (260 µL, 4.40 mmol, 4 eq) and **2** (305 mg, 1.10 mmol, 1 eq). The resulting mixture was stirred under reflux for 48 h and H_2O (20 mL) was added. The layers were separated and the aqueous layer was extracted with toluene (2 × 10 mL). The organic layers were combined, washed with a saturated aqueous solution of $NaHCO_3$ (10 mL), dried over anhydrous sodium sulfate, and evaporated under vacuum. The crude product was purified by flash chromatography (silica gel-petroleum ether/ethyl acetate: 8/2) to afford **3** (350 mg, 1.00 mmol, 90%). Orange crystalline solid; R_f: 0.30 (petroleum ether/ethyl acetate: 8/2); Mp: 105°C (*litt*.[66] 129°C); IR: 3251, 1597, 1478, 1389, 1336, 1167, 1092, 911, 772, 693 cm^{-1}; ^1H NMR (400 MHz, $(CD_3)_2CO$): δ 9.71 (br s, 1H), 7.89 (m, 2H), 7.76 (d, J = 9.2 Hz, 1H), 7.69-7.66 (m, 3H), 7.60-7.58 (m, 3H), 7.53 (t, J = 7.8 Hz, 1H), 7.25 (t, J = 7.8 Hz, 1H), 7.16 (d, J = 7.8 Hz, 2H), 2.22 (s, 3H); $^{13}C\{^1H\}$ NMR (100 MHz, $(CD_3)_2CO$): δ 153.1, 144.7, 142.9, 137.6, 136.7, 133.3, 132.5, 130.3, 130.1, 127.9, 125.9, 123.9, 123.5, 119.8, 21.3.

Complex 4. To a solution of **3** (80 mg, 0.23 mmol) in 10 mL of MeOH were added Et_3N (62 µL, 0.46 mmol) and $[Ru(p\text{-cym})Cl_2]_2$ (70 mg, 0.11 mmol). After stirring for 24 h the precipitate was filtered and washed with Et_2O to afford **4** (112 mg, 0.180 mmol, 78%). Brown powder; R_f: 0.73 (CH_2Cl_2/MeOH: 95/5); Mp: 244°C; IR: 2969, 1596, 1474, 1305, 1142, 1082, 932, 851, 763, 697 cm^{-1}; ^1H NMR (400 MHz, $CDCl_3$): δ 8.09 (d, J = 8.2 Hz, 2H), 7.86 (m, 3H), 7.64 (t, J = 7.8 Hz, 2H), 7.52 (m, 1H), 7.38 (d, J = 8.7 Hz, 1H), 7.15 (d, J = 8.2 Hz, 2H), 7.04 (t, J = 8.4 Hz, 1H), 6.60 (t, J = 7.6 Hz, 1H), 6.32 (br s, 1H), 5.43 (d, J = 6.0 Hz, 1H), 5.05 (d, J = 5.5 Hz, 1H), 3.74 (br s, 1H), 2.67 (sept, J = 6.9 Hz, 1H), 2.31 (s, 3H), 2.15 (s, 3H), 1.08 (d, J = 6.9 Hz, 3H), 0.87 (d, J = 6.9 Hz, 3H); $^{13}C\{^1H\}$ NMR (100 MHz, $CDCl_3$): δ 156.0, 151.6, 148.5, 142.1, 137.9, 133.3, 129.3, 128.9, 128.7, 122.5, 119.6, 119.0, 118.4, 82.9, 82.5, 31.0, 23.6, 21.6, 21.2, 19.3; HRMS (ESI) calcd. for $C_{29}H_{30}N_3O_2RuS^+$, $[M - Cl]^+$ m/z 586.1104, found m/z 586.1106; Anal. calcd. for $C_{29}H_{30}N_3O_2RuSCl$, C: 56.08, H: 4.87, N: 6.76, found C: 56.11, H: 4.95, N: 6.61.

(*E*)-2-(Methanesulfonamido)azobenzene **6**. To a solution of **5**[53] (50 mg, 0.25 mmol) in pyridine (5 mL) was added methanesulfonyl chloride (22 µL, 0.28 mmol, 1.1 eq). Stirring at room temperature for 12 h was followed by addition of another portion of methanesulfonyl chloride (22 µL, 0.28 mmol, 1.1 eq). After completion, the mixture was evaporated to dryness. CH_2Cl_2 (20 mL) and H_2O (20 mL) were added, the layers were separated and the aqueous layer was extracted with CH_2Cl_2 (3 × 10 mL). The organic layers were combined, washed with a saturated aqueous solution of NH_4Cl (10 mL), dried over anhydrous sodium sulfate, and evaporated under vacuum. The crude product was purified by flash chromatography (silica gel-petroleum ether/ethyl acetate: 8/2) to afford **6** (57 mg, 0.21 mmol, 82%). Orange crystalline solid; R_f: 0.34 (petroleum ether/ethyl acetate: 8/2); Mp: 100°C; IR: 3270, 1595, 1484,1375, 1335, 1166, 1152, 971, 773, 732, 690 cm^{-1}; ^1H NMR (400 MHz, $(CD_3)_2CO$): δ 9.52 (br s, 1H), 8.00 (m, 2H), 7.87 (dd, J = 8.0, 1.6 Hz, 1H), 7.79 (m, 1H), 7.62-7.56 (m, 4H), 7.31 (ddd, J = 8.4, 7.2, 1.4 Hz, 1H), 3.15 (s, 3H); $^{13}C\{^1H\}$ NMR (100 MHz, $(CD_3)_2CO$): δ 153.2, 141.8, 137.3, 133.7, 132.6, 130.2, 125.1, 123.9, 121.4, 120.4, 40.2; HRMS (ESI) calcd. for $C_{13}H_{13}N_3O_2SNa^+$, $[M + Na]^+$ m/z 298.0626, found m/z 298.0629.

Complex 7. To a solution of **6** (19 mg, 0.066 mmol) in 4 mL of MeOH were added Et_3N (18 µL, 0.13 mmol) and $[Ru(p\text{-cym})Cl_2]_2$ (20 mg, 0.033 mmol). After stirring for 24 h the mixture was evaporated to dryness and the product was purified by flash chromatography (silica gel-CH_2Cl_2/MeOH: 250/2 to 250/4) to afford **7** (23 mg, 0.042 mmol, 63%). Black powder; R_f: 0.58 (CH_2Cl_2/MeOH: 95/5); Mp: 189°C; IR: 3477, 1593, 1468, 1300, 1241, 1126, 960, 926, 845, 733, 679 cm^{-1}; ^1H NMR (400 MHz, $CDCl_3$): δ 8.09 (d, J = 8.7 Hz, 1H), 7.95 (dd, J = 8.5, 1.1 Hz, 1H), 7.75 (d, J = 7.8 Hz, 2H), 7.61 (t, J = 7.8 Hz, 2H), 7.50 (m, 1H), 7.34 (m, 1H), 6.76 (m, 1H), 6.20 (br s, 1H), 5.33 (d, J = 6.0 Hz, 1H), 5.02 (d, J = 5.5 Hz, 1H), 3.51 (br s, 1H), 3.12 (s, 3H), 2.56 (sept, J = 6.9 Hz, 1H), 2.11 (s, 3H), 1.07 (d, J = 6.9 Hz, 3H), 0.89 (d, J = 6.9 Hz, 3H); $^{13}C\{^1H\}$ NMR (100 MHz, $CDCl_3$): δ 156.4, 152.4, 149.3, 134.1, 129.0, 128.6, 122.1, 119.8, 119.0, 83.0, 82.8, 41.0, 31.0, 23.3, 21.5, 19.2; HRMS (ESI) calcd. for $C_{23}H_{27}N_3O_2RuS^+$, $[M - Cl]^+$ m/z 510.0789, found m/z 510.0789; Anal. calcd. for $C_{23}H_{27}N_3O_2RuSCl$, C: 50.68, H: 4.81, N: 7.71, found C: 50.35, H: 4.73, N: 7.34.

(*E*)-2-(Trifluoromethanesulfonamido)azobenzene **8.** To a solution of **5** (208 mg, 1.05 mmol) in dry CH_2Cl_2 (20 mL) under argon was added trifluoromethanesulfonic acid (196 µL, 1.16 mmol, 1.1 eq). The mixture was stirred at room temperature for 10 min before addition of H_2O (20 mL). The layers were separated and the aqueous layer was extracted with CH_2Cl_2 (3 × 20 mL). The organic layers were combined, washed with brine (10 mL), dried over anhydrous sodium sulfate, and finally, evaporated under vacuum. **8** (325 mg, 94%) was used without further purification. A small portion for analysis was purified by flash chromatography (silica gel-petroleum ether/ethyl acetate: 98/2). Orange crystalline solid; R_f: 0.58 (petroleum ether/ethyl acetate: 8/2); Mp: 76°C; IR: 3264, 1597, 1485, 1415, 1214, 1193, 1140, 957, 770, 684 cm^{-1}; ^1H NMR (400 MHz, $(CD_3)_2CO$): δ 10.71 (br s, 1H), 8.03 (dd, J = 7.8, 1.8 Hz, 2H), 7.86 (dd, J = 8.0, 1.6 Hz, 1H), 7.75 (m, 1H), 7.67 (m, 1H), 7.62-7.60 (m, 3H), 7.53 (m, 1H); $^{13}C\{^1H\}$ NMR (100 MHz, $(CD_3)_2CO$): δ 153.4, 146.0, 134.5, 133.3, 132.9, 130.2, 128.9, 127.1, 124.2, 117.8; HRMS (ESI) calcd. for $C_{13}H_{11}F_3N_3O_2S^+$, $[M + H]^+$ m/z 330.0519, found m/z 330.0519.

Complex 9. A solution of **8** (108 mg, 0.328 mmol) in 10 mL of MeOH and $[Ru(p\text{-cym})Cl_2]_2$ (100 mg, 0.215 mmol) was stirred for 48 h and evaporated to dryness. The product was purified by flash chromatography (silica gel-CH_2Cl_2/MeOH: 250/2 to 250/5) to afford **9** (58 mg, 0.097 mmol, 29%). Dark red powder; R_f: 0.77 (CH_2Cl_2/MeOH: 95/5); Mp: 245°C; IR: 3057, 1598, 1476, 1353, 1203, 1179, 1162, 1134, 949, 838, 767, 694 cm^{-1}; ^1H NMR (400 MHz, $CDCl_3$): δ 8.11-7.77 (br s, 1H), 7.97 (d, J = 8.7 Hz, 1H), 7.86 (d, J = 7.8 Hz, 2H), 7.65 (m, 2H), 7.54 (m, 1H), 7.37 (ddd, J = 8.6, 7.0, 1.4 Hz, 1H), 6.91 (m, 1H), 6.03-3.98 (7 br s, 1H), 2.49 (br s, 1H), 2.39-2.08 (m, 3H), 1.07-0.83 (m, 6H); $^{13}C\{^1H\}$ NMR (100 MHz, $CDCl_3$): δ 155.8 (br), 149.6, 149.1, 133.7, 129.3, 129.2, 122.1, 121.9, 120.7 (br), 118.7, 108.5 (br), 102.5 (br), 92.1 (br), 89.0 (br), 86.0 (br), 85.1 (br), 83.5-82.5 (br), 66.0, 31.1, 30.0, 22.9-21.6 (br), 19.2, 15.4; HRMS (ESI) calcd. for $C_{23}H_{23}F_3N_3O_2RuS^+$, $[M - Cl]^+$ m/z 564.0507, found m/z 564.0519; Anal. calcd. for $C_{23}H_{23}ClF_3N_3O_2RuS$, C: 46.12, H: 3.87, N: 7.01, found C: 46.36, H: 4.13, N: 7.05.

2,6-Difluoronitrosobenzene 10. To a solution of 2,6-difluoroaniline (500 µL, 4.65 mmol) in CH_2Cl_2 (15 mL) was added dropwise a solution of Oxone® (5.71 g, 9.29 mmol, 2 eq) in 15 mL H_2O. The resulting mixture was vigorously stirred at room temperature for 15 h. The layers were separated and the aqueous layer was extracted with CH_2Cl_2 (2 × 5 mL). The organic layers were combined, washed with a saturated aqueous solution of $NaHCO_3$ (10 mL), dried over anhydrous sodium sulfate and evaporated under vacuum to afford **10** (660 mg, 4.61 mmol, 99%). Light brown powder; R_f: 0.55 (petroleum ether/ethyl acetate: 8/2); Mp: 119°C; IR: 3662, 3225, 2986, 2901, 1608, 1478, 1283, 1163, 1086, 1019, 914, 788 cm^{-1}; ^1H NMR (400 MHz, $(CD_3)_2CO$): δ 7.92 (m, 1H), 7.37 (t, J = 8.9 Hz, 2H); $^{13}C\{^1H\}$ NMR (100 MHz, $(CD_3)_2CO$): δ 154.2 (d, J = 267 Hz), 139.6 (t, J = 11.4 Hz), 114.1 (d, J = 23.8 Hz).

(*E*)-2-(4-Methylphenylsulfonamido)-2',6'-difluoroazobenzene **11.** To a solution of **1** (92 mg, 0.35 mmol) in acetic acid (5 mL) was added **10** (50 mg, 0.35 mmol, 1 eq). The resulting mixture was stirred under reflux for 16 h and evaporated

to dryness under vacuum. The crude product was purified by flash chromatography (silica gel-petroleum ether/ethyl acetate: 9/1) to afford **11** (33 mg, 0.085 mmol, 24%). Orange crystalline solid; R_f: 0.39 (petroleum ether/ethyl acetate: 8/2); Mp: 140°C; IR: 3299, 1613, 1594, 1477, 1390, 1338, 1165, 1092, 1028, 926, 759 cm^{-1}; ^1H NMR (400 MHz, $CDCl_3$): δ 9.20 (s, 1H); 7.79 (d, J = 8.2 Hz, 1H), 7.72-7.69 (m, 3H), 7.44 (m, 1H), 7.40 (ddd, J = 8.5, 6.0, 2.5 Hz, 1H), 7.17-7.06 (m, 5H), 2.33 (s, 3H); $^{13}C\{^1H\}$ NMR (100 MHz, $CDCl_3$): δ 156.3 (d, J = 259 Hz), 144.2, 141.0, 136.2, 136.1, 133.9, 131.4 (t, J = 10.5 Hz), 129.8, 127.4, 124.2, 119.9, 119.8, 112.9, 21.6; HRMS (ESI) calcd. for $C_{19}H_{15}F_2N_3O_2SNa^+$, $[M + Na]^+$ m/z 410.0751, found m/z 410.0748.

Complex 12. To a solution of **11** (97 mg, 0.26 mmol) in 10 mL of MeOH were added Et_3N (70 µL, 0.52 mmol) and $[Ru(p\text{-cym})Cl_2]_2$ (80 mg, 0.13 mmol). After stirring for 24 h the mixture was evaporated to dryness and the product was purified by flash chromatography (silica gel-CH_2Cl_2/MeOH: 250/3) to afford **12** (93 mg, 0.14 mmol, 57%). Black powder; R_f: 0.65 (CH_2Cl_2/MeOH: 95/5); Mp: 245°C; IR: 3738, 2967, 1712, 1595, 1469, 1400, 1308, 1245, 1139, 1081, 1007, 924, 849, 787 cm^{-1}; ^1H NMR (400 MHz, $CDCl_3$): δ 8.08 (d, J = 7.8 Hz, 2H), 7.69 (d, J = 8.2 Hz, 1H), 7.43-7.37 (m, 2H), 7.20-7.05 (m, 5H), 6.91 (m, 1H), 6.60 (t, J = 7.8 Hz, 1H), 5.51-5.46 (m, 2H), 3.66 (br s, 1H), 2.83 (m, 1H), 2.27 (s, 3H), 1.99 (s, 3H), 1.19 (br s, 3H), 0.87 (br s, 3H); $^{13}C\{^1H\}$ NMR (100 MHz, $CDCl_3$): δ 151.0 (d, J = 237 Hz), 142.2, 137.4, 134.2, 133.6, 129.3, 129.0, 128.6 (t, J = 91 Hz), 119.3, 119.2, 118.8, 111.7 (br), 100.1, 97.3, 83.2, 81.8, 78.7, 53.6, 31.2, 31.1, 24.5, 21.6, 20.5, 19.8; HRMS (ESI) calcd. for $C_{29}H_{28}F_2N_3O_2RuS^+$, $[M - Cl]^+$ m/z 622.0915, found m/z 622.0918; Anal. calcd. for $C_{29}H_{28}ClF_2N_3O_2RuS$, C: 53.01, H: 4.29, N: 6.39, found C: 52.22, H: 4.59, N: 5.70.

Complex 13. To a solution of **3** (71 mg, 0.20 mmol) in 5 mL of MeOH were added Et_3N (55 µL, 0.40 mmol) and $[Ru(bz)Cl_2]_2$ (50 mg, 0.10 mmol). After stirring for 2 h the precipitate was filtered and washed with MeOH and Et_2O to afford **13** (94 mg, 0.13 mmol, 83%).

Brown powder; R_f: 0.42 (CH_2Cl_2/MeOH: 95/5); Mp: > 270°C; IR: 3070, 1596, 1472, 1299, 1155, 1135, 1084, 939, 908, 848, 821, 767, 695 cm^{-1}; ^1H NMR (400 MHz, $CDCl_3$): δ 8.09 (d, J = 8.2 Hz, 2H), 7.88-7.85 (m, 3H), 7.66 (t, J = 7.6 Hz, 2H), 7.54 (m, 1H), 7.41 (d, J = 8.7 Hz, 1H), 7.17 (d, J = 7.8 Hz, 2H), 7.07 (t, J = 7.8 Hz, 1H), 6.63 (t, J = 7.8 Hz, 1H), 5.48 (s, 6H), 2.32 (s, 3H); $^{13}C\{^1H\}$ NMR (100 MHz, $CDCl_3$): δ 155.7, 152.0, 148.7, 142.3, 137.7, 133.5, 129.3, 129.0, 128.9, 122.4, 119.6, 119.2, 118.7, 87.2, 21.6; HRMS (ESI) calcd. for $C_{25}H_{22}N_3O_2RuS^+$, $[M - Cl]^+$ m/z 530.0477, found m/z 530.0476; Anal. calc. for $C_{25}H_{22}ClN_3O_2RuS$, C: 53.14, H: 3.92, N: 6.27, found C: 52.59, H: 4.11, N: 7.37.

Complex 14. To a solution of **3** (32 mg, 0.09 mmol) in 3 mL of MeOH were added Et_3N (25 µL, 0.18 mmol) and $[Ru(hmbz)Cl_2]_2$ (30 mg, 0.045 mmol). After stirring for 15 h the precipitate was filtered and washed with MeOH and Et_2O to afford **14** (44 mg, 0.068 mmol, 75%). Black powder; R_f: 0.46 (CH_2Cl_2/MeOH: 95/5); Mp: 264°C; IR: 3736, 3051, 1593, 1470, 1301, 1137, 1085, 934, 850, 767, 679 cm^{-1}; ^1H NMR (400 MHz, $CDCl_3$): δ 8.56 (d, J = 7.8 Hz, 2H), 7.96 (d, J = 8.7 Hz, 2H), 7.91 (d, J = 8.2 Hz, 1H), 7.72 (d, J = 8.7 Hz, 1H), 7.68-7.64 (m, 2H), 7.46 (t, J = 7.6 Hz, 1H), 7.08-7.02 (m, 3H), 6.61 (m, 1H), 2.24 (s, 3H), 1.83 (s, 18H); $^{13}C\{^1H\}$ NMR (100 MHz, $CDCl_3$): δ 152.6, 151.5, 150.7, 141.5, 139.0, 131.9, 130.4, 129.6, 129.2, 128.9, 124.8, 120.6, 118.9, 117.7, 96.2, 21.5, 16.1; HRMS (ESI) calcd. for $C_{31}H_{34}N_3O_2RuS^+$, $[M - Cl]^+$ m/z 614.1417, found m/z 614.1414; Anal. calc. for $C_{31}H_{34}ClN_3O_2RuS$, C: 57.35, H: 5.28, N: 6.47, found C: 57.12, H: 5.36, N: 6.46.

Computational Details. All density functional theory (DFT) calculations were performed with Gaussian09 package at the B3LYP level.[65] LanL2DZ and 6-31G**(d,p) basis sets were used for Ru and all other atoms, respectively. The effect of solvent (acetonitrile) was taken into account by continuum CPCM single point calculation on gas-phase optimized geometries. The absence of imaginary frequencies was checked on all calculated structures to confirm they are true minima.

ASSOCIATED CONTENT

Supporting Information

Copy of NMR spectra, additional UV-vis absorption spectra, procedures for the determination of half-lives and (*Z*)/(*E*) ratio in the PSS, details concerning X-ray structure determination and a text file of all computed molecule Cartesian coordinates in a format for convenient visualization. This material is available free of charge via the Internet at http://pubs.acs.org.

AUTHOR INFORMATION

Note

The authors declare no competing financial interest.

Corresponding Author

* E-mail: nicolas.bogliotti@ppsm.ens-cachan.fr, joanne.xie@ens-cachan.fr

ACKNOWLEDGMENT

We thank Dr. Gilles Clavier for helpful discussions concerning DFT calculations.

REFERENCES

(1) Hu, Y.; Tabor, R. F.; Wilkinson, B. L. *Org. Biomol. Chem.* **2015**, *13*, 2216–2225.

(2) Velema, W. A.; Szymanski, W.; Feringa, B. L. *J. Am. Chem. Soc.* **2014**, *136*, 2178–2191.

(3) Li, J.; Wang, X.; Liang, X. *Chem. - Asian J.* **2014**, *9*, 3344–3358.

(4) Kundu, P. K.; Klajn, R. *ACS Nano* **2014**, *8*, 11913–11916.

(5) García-Iriepa, C.; Marazzi, M.; Frutos, L. M.; Sampedro, D. *RSC Adv.* **2013**, *3*, 6241–6266.

(6) Wegner, H. A. *Angew. Chem. Int. Ed.* **2012**, *51*, 4787–4788.

(7) Bandara, H. M. D.; Burdette, S. C. *Chem. Soc. Rev.* **2012**, *41*, 1809–1825.

(8) Merino, E. *Chem. Soc. Rev.* **2011**, *40*, 3835–3853.

(9) Beharry, A. A.; Woolley, G. A. *Chem. Soc. Rev.* **2011**, *40*, 4422–4437.

(10) Hamon, F.; Djedaini-Pilard, F.; Barbot, F.; Len, C. *Tetrahedron* **2009**, *65*, 10105–10123.

(11) Samanta, S.; Ghosh, P.; Goswami, S. *Dalton Trans.* **2012**, *41*, 2213–2226.

(12) Pattanayak, P.; Parua, S. P.; Patra, D.; Lai, C.-K.; Brandão, P.; Felix, V.; Chattopadhyay, S. *Inorganica Chim. Acta* **2015**, *429*, 122–131.

(13) Ding, F.; Sun, Y.; Verpoort, F. *Eur. J. Inorg. Chem.* **2010**, *2010*, 1536–1543.

(14) Kannan, S.; Ramesh, R.; Liu, Y. *J. Organomet. Chem.* **2007**, *692*, 3380–3391.

(15) Venkatachalam, G.; Ramesh, R. *Tetrahedron Lett.* **2005**, *46*, 5215–5218.

(16) Rath, R. K.; Nethaji, M.; Chakravarty, A. R. *J. Organomet. Chem.* **2001**, *633*, 79–84.

(17) Romero-Canelón, I.; Salassa, L.; Sadler, P. J. *J. Med. Chem.* **2013**, *56*, 1291–1300.

(18) Dougan, S. J.; Habtemariam, A.; McHale, S. E.; Parsons, S.; Sadler, P. J. *Proc. Natl. Acad. Sci.* **2008**, *105*, 11628–11633.

(19) Velders, A. H.; Kooijman, H.; Spek, A. L.; Haasnoot, J. G.; de Vos, D.; Reedijk, J. *Inorg. Chem.* **2000**, *39*, 2966–2967.

(20) Dougan, S. J.; Melchart, M.; Habtemariam, A.; Parsons, S.; Sadler, P. J. *Inorg. Chem.* **2006**, *45*, 10882–10894.

(21) Dinda, J.; Senapoti, S.; Mondal, T.; Jana, A. D.; Chiang, M. Y.; Lu, T.-H.; Sinha, C. *Polyhedron* **2006**, *25*, 1125–1132.

(22) Govindaswamy, P.; Sinha, C.; Kollipara, M. R. *J. Organomet. Chem.* **2005**, *690*, 3465–3473.

(23) Velders, A. H.; van der Schilden, K.; Hotze, A. C.; Reedijk, J.; Kooijman, H.; Spek, A. L. *Dalton Trans.* **2004**, 448–455.

(24) Das, C.; Saha, A.; Hung, C.-H.; Lee, G.-H.; Peng, S.-M.; Goswami, S. *Inorg. Chem.* **2003**, *42*, 198–204.

(25) Das, C.; Ghosh, A. K.; Hung, C.-H.; Lee, G.-H.; Peng, S.-M.; Goswami, S. *Inorg. Chem.* **2002**, *41*, 7125–7135.

(26) Flower, K. R.; Pritchard, R. G. *J. Organomet. Chem.* **2001**, *620*, 60–68.

(27) Rath, R. K.; Valavi, S. G.; Geetha, K.; Chakravarty, A. R. *J. Organomet. Chem.* **2000**, *596*, 232–236.

(28) Mondal, B.; Walawalkar, M. G.; Kumar Lahiri, G. *J. Chem. Soc. Dalton Trans.* **2000**, 4209–4217.

(29) Hotze, A. C. G.; Velders, A. H.; Ugozzoli, F.; Biagini-Cingi, M.; Manotti-Lanfredi, A. M.; Haasnoot, J. G.; Reedijk, J. *Inorg. Chem.* **2000**, *39*, 3838–3844.

(30) Santra, P. K.; Misra, T. K.; Das, D.; Sinha, C.; Slawin, A. M.; Woollins, J. D. *Polyhedron* **1999**, *18*, 2869–2878.

(31) Pattanayak, P.; Patra, D.; Pratihar, J. L.; Burrows, A.; Mahon, M. F.; Chattopadhyay, S. *Inorganica Chim. Acta* **2010**, *363*, 2865–2873.

(32) Pratihar, J. L.; Bhaduri, S.; Pattanayak, P.; Patra, D.; Chattopadhyay, S. *J. Organomet. Chem.* **2009**, *694*, 3401–3408.

(33) Samanta, S.; Singh, P.; Fiedler, J.; Záliš, S.; Kaim, W.; Goswami, S. *Inorg. Chem.* **2008**, *47*, 1625–1633.

(34) Kitaura, R.; Miyaki, Y.; Onishi, T.; Kurosawa, H. *Inorganica Chim. Acta* **2002**, *334*, 142–148.

(35) Miyaki, Y.; Onishi, T.; Kurosawa, H. *Chem. Lett.* **2000**, *29*, 1334–1335.

(36) Corrigan, J. F.; Doherty, S.; Taylor, N. J.; Carty, A. J. *J. Chem. Soc. Chem. Commun.* **1991**, 1640–1641.

(37) Kume, S.; Nishihara, H. *Dalton Trans.* **2008**, 3260–3271.

(38) Amar, A.; Savel, P.; Akdas-Kilig, H.; Katan, C.; Meghezzi, H.; Boucekkine, A.; Malval, J.-P.; Fillaut, J.-L. *Chem. - Eur. J.* **2015**, *21*, 8262–8270.

(39) Göstl, R.; Senf, A.; Hecht, S. *Chem. Soc. Rev.* **2014**, *43*, 1982–1996.

(40) Lee, H.-M.; Larson, D. R.; Lawrence, D. S. *ACS Chem. Biol.* **2009**, *4*, 409–427.

(41) Lüning, U. *Angew. Chem. Int. Ed.* **2012**, *51*, 8163–8165.

(42) Akita, M. *Organometallics* **2011**, *30*, 43–51.

(43) Stoll, R. S.; Hecht, S. *Angew. Chem. Int. Ed.* **2010**, *49*, 5054–5075.

(44) Samachetty, H. D.; Branda, N. R. *Pure Appl. Chem.* **2006**, *78*, 2351–2359.

(45) Szymański, W.; Beierle, J. M.; Kistemaker, H. A. V.; Velema, W. A.; Feringa, B. L. *Chem. Rev.* **2013**, *113*, 6114–6178.

(46) Brieke, C.; Rohrbach, F.; Gottschalk, A.; Mayer, G.; Heckel, A. *Angew. Chem. Int. Ed.* **2012**, *51*, 8446–8476.

(47) Mayer, G.; Heckel, A. *Angew. Chem. Int. Ed.* **2006**, *45*, 4900–4921.

(48) Wang, H.; Yu, Y.; Hong, X.; Tan, Q.; Xu, B. *J. Org. Chem.* **2014**, *79*, 3279–3288.

(49) Rivillo, D.; Gulyás, H.; Benet-Buchholz, J.; Escudero-Adán, E. C.; Freixa, Z.; van Leeuwen, P. W. N. M. *Angew. Chem. Int. Ed.* **2007**, *46*, 7247–7250.

(50) Brown, E. V.; Granneman, G. R. *J. Am. Chem. Soc.* **1975**, *97*, 621–627.

(51) Knie, C.; Utecht, M.; Zhao, F.; Kulla, H.; Kovalenko, S.; Brouwer, A. M.; Saalfrank, P.; Hecht, S.; Bléger, D. *Chem. - Eur. J.* **2014**, *20*, 16492–16501.

(52) Bléger, D.; Schwarz, J.; Brouwer, A. M.; Hecht, S. *J. Am. Chem. Soc.* **2012**, *134*, 20597–20600.

(53) Bellotto, S.; Reuter, R.; Heinis, C.; Wegner, H. A. *J. Org. Chem.* **2011**, *76*, 9826–9834.

(54) Martínez-Alonso, M.; Busto, N.; Jalón, F. A.; Manzano, B. R.; Leal, J. M.; Rodríguez, A. M.; García, B.; Espino, G. *Inorg. Chem.* **2014**, *53*, 11274–11288.

(55) Bugarcic, T.; Habtemariam, A.; Deeth, R. J.; Fabbiani, F. P. A.; Parsons, S.; Sadler, P. J. *Inorg. Chem.* **2009**, *48*, 9444–9453.

(56) Giannini, F.; Geiser, L.; Paul, L. E. H.; Roder, T.; Therrien, B.; Süss-Fink, G.; Furrer, J. *J. Organomet. Chem.* **2015**, *783*, 40–45.

(57) Štěpnička, P.; Ludvík, J.; Canivet, J.; Süss-Fink, G. *Inorganica Chim. Acta* **2006**, *359*, 2369–2374.

(58) Canivet, J.; Labat, G.; Stoeckli-Evans, H.; Süss-Fink, G. *Eur. J. Inorg. Chem.* **2005**, *2005*, 4493–4500.

(59) Canivet, J.; Karmazin-Brelot, L.; Süss-Fink, G. *J. Organomet. Chem.* **2005**, *690*, 3202–3211.

(60) Reichardt, C. In *Solvents and Solvent Effects in Organic Chemistry*; Wiley-VCH Verlag GmbH & Co. KGaA, 2003; pp 389–469.

(61) Reichardt, C. *Pure Appl. Chem.* **1982**, *54*, 1867–1884.

(62) Reichardt, C. In *Solvents and Solvent Effects in Organic Chemistry*; Wiley-VCH Verlag GmbH & Co. KGaA, 2003; pp 147–328.

(63) Hansch, C.; Leo, A.; Taft, R. W. *Chem. Rev.* **1991**, *91*, 165–195.

(64) Stang, P. J.; Anderson, A. G. *J. Org. Chem.* **1976**, *41*, 781–785.

(65) Frisch, M. J.; Trucks, G. W.; Schlegel, H. B.; Scuseria, G. E.; Robb, M. A.; Cheeseman, J. R.; Scalmani, G.; Barone, V.; Mennucci, B.; Petersson, G. A.; Nakatsuji, H.; Caricato, M.; Li, X.; Hratchian, H. P.; Izmaylov, A. F.; Bloino, J.; Zheng, G.; Sonnenberg, J. L.; Hada, M.; Ehara, M.; Toyota, K.; Fukuda, R.; Hasegawa, J.; Ishida, M.; Nakajima, T.; Honda, Y.; Kitao, O.; Nakai, H.; Vreven, T.; Montgomery Jr., J. A.; Peralta, J. E.; Ogliaro, F.; Bearpark, M. J.; Heyd, J.; Brothers, E. N.; Kudin, K. N.; Staroverov, V. N.; Kobayashi, R.; Normand, J.; Raghavachari, K.; Rendell, A. P.;

Burant, J. C.; Iyengar, S. S.; Tomasi, J.; Cossi, M.; Rega, N.; Millam, N. J.; Klene, M.; Knox, J. E.; Cross, J. B.; Bakken, V.; Adamo, C.; Jaramillo, J.; Gomperts, R.; Stratmann, R. E.; Yazyev, O.; Austin, A. J.; Cammi, R.; Pomelli, C.; Ochterski, J. W.; Martin, R. L.; Morokuma, K.; Zakrzewski, V. G.; Voth, G. A.; Salvador, P.; Dannenberg, J. J.; Dapprich, S.; Daniels, A. D.; Farkas, Ö.; Foresman, J. B.; Ortiz, J. V.; Cioslowski, J.; Fox, D. J. *Gaussian 09*; Gaussian, Inc.: Wallingford, CT, USA, 2009.

(66) Jia, X.; Han, J. *J. Org. Chem.* **2014**, *79*, 4180–4185.

Insert Table of Contents artwork here

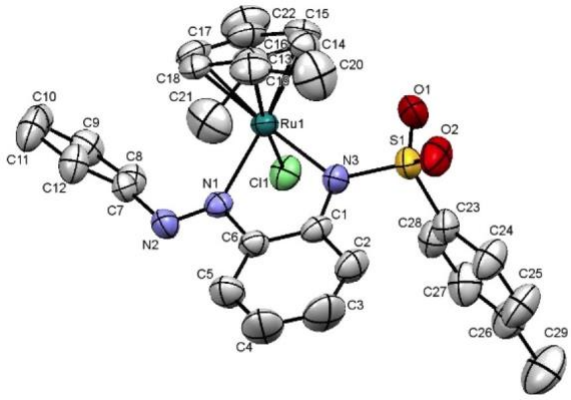

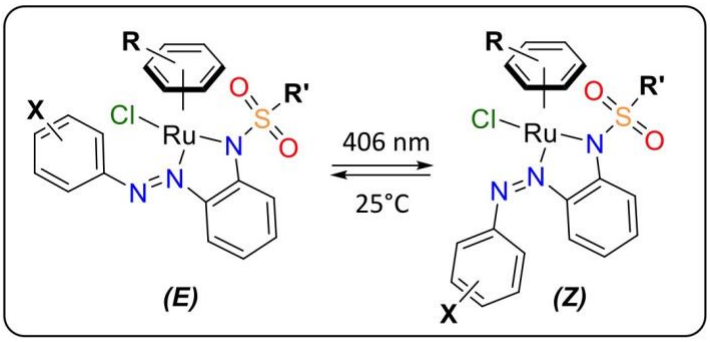

Exocyclic N=N bond